Supplementary information

An advanced three–dimensionally ordered macroporous $NiCo_2O_4$ spinel as bifunctional electrocatalyst for rechargeable Zn–Air batteries

José Béjar,[1,] Lorena Álvarez-Contreras,[2] J. Ledesma-García,[3] Noé Arjona[1] and L. G. Arriaga[1]***

[1]Centro de Investigación y Desarrollo Tecnológico en Electroquímica S. C., Querétaro, C. P. 76703, México.

[2]Centro de Investigación en Materiales Avanzados S. C., Complejo Industrial Chihuahua, Chihuahua, C. P. 31136, México.

[3]Facultad de Ingeniería, División de Investigación y Posgrado, Universidad Autónoma de Querétaro, Querétaro, C. P. 76010, México

Corresponding authors:

**noe.arjona@yahoo.com.mx & wvelazquez@cideteq.mx. Tel: +52 (442) 211 60 00 ext. 7874*

***larriaga@cideteq.mx; Tel: +52 (442) 211 60 69*

S1. Synthesis of PMMA microspheres.

CCT was synthetized by the microemulsion of methyl methacrylate monomer. First, 100 ml of distilled water was placed in a three-neck flask and stirred at 350 rpm. In the meantime, 38 mg sodium dodecyl sulphate (Sigma Aldrich) was dispersed in 5 ml water and added into the flask. At this time, a flow of nitrogen (90 ml min^{-1}) was incorporated and maintained throughout the process. Afterwards, the solution was heated at 70°C, and at this point, 40 ml MMA (Across organics) was added to the solution. Then, 15 minutes later, 350 mg ammonium persulfate (Sigma Aldrich 98 %) dispersed in 5 ml water was incorporated into the solution. Stirring and heating were maintained for 4 hours. The next step was to assemble the spheres into close-packed arrays. First, 10 millilitres of the latex were poured into a vial and centrifuged for 3 hours at 4000 rpm. Finally, the template was dried at 60°C for 12 hours. Finally, uniform disks 3.5 cm in diameter with a thickness of 0.5 cm were obtained.

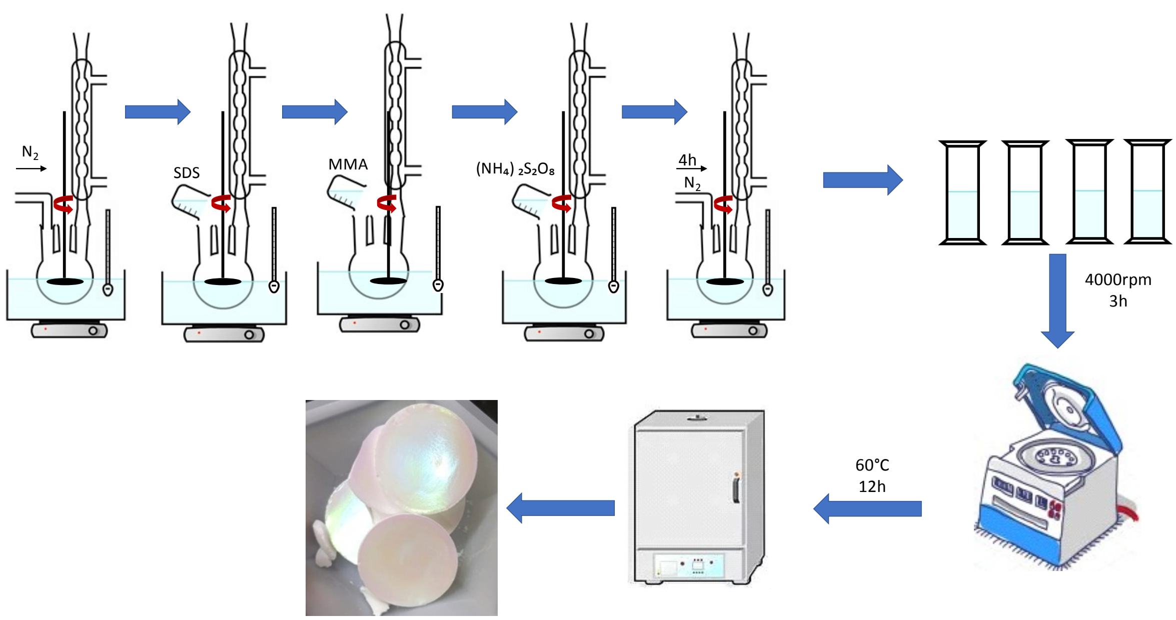

Figure S1. Methodology for the synthesis of PMMA microspheres by emulsion polymerization and CCT assembly.

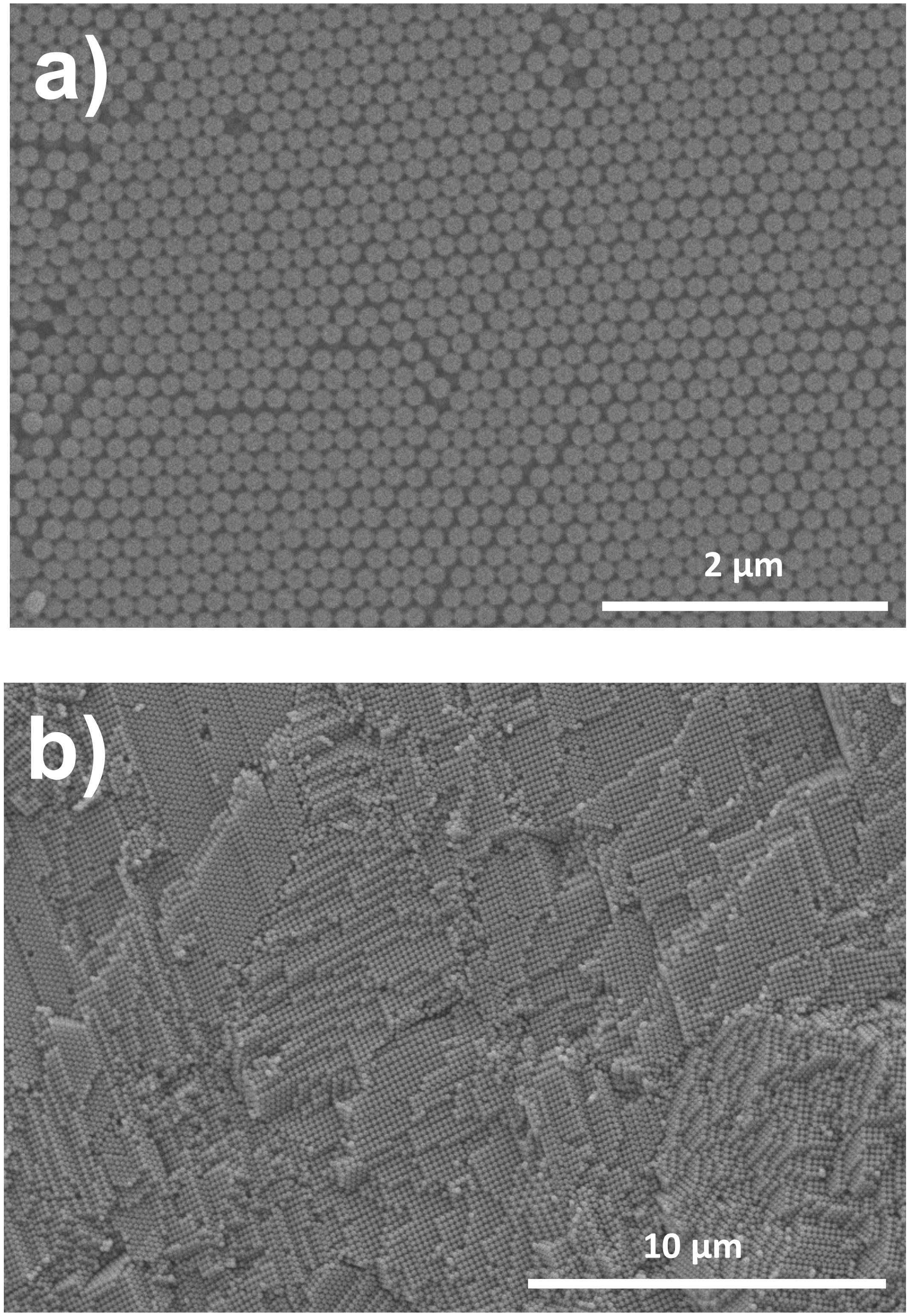

Figure S2. SEM micrographs of the PMMA CCT: a) the surface part and b) the inner part.

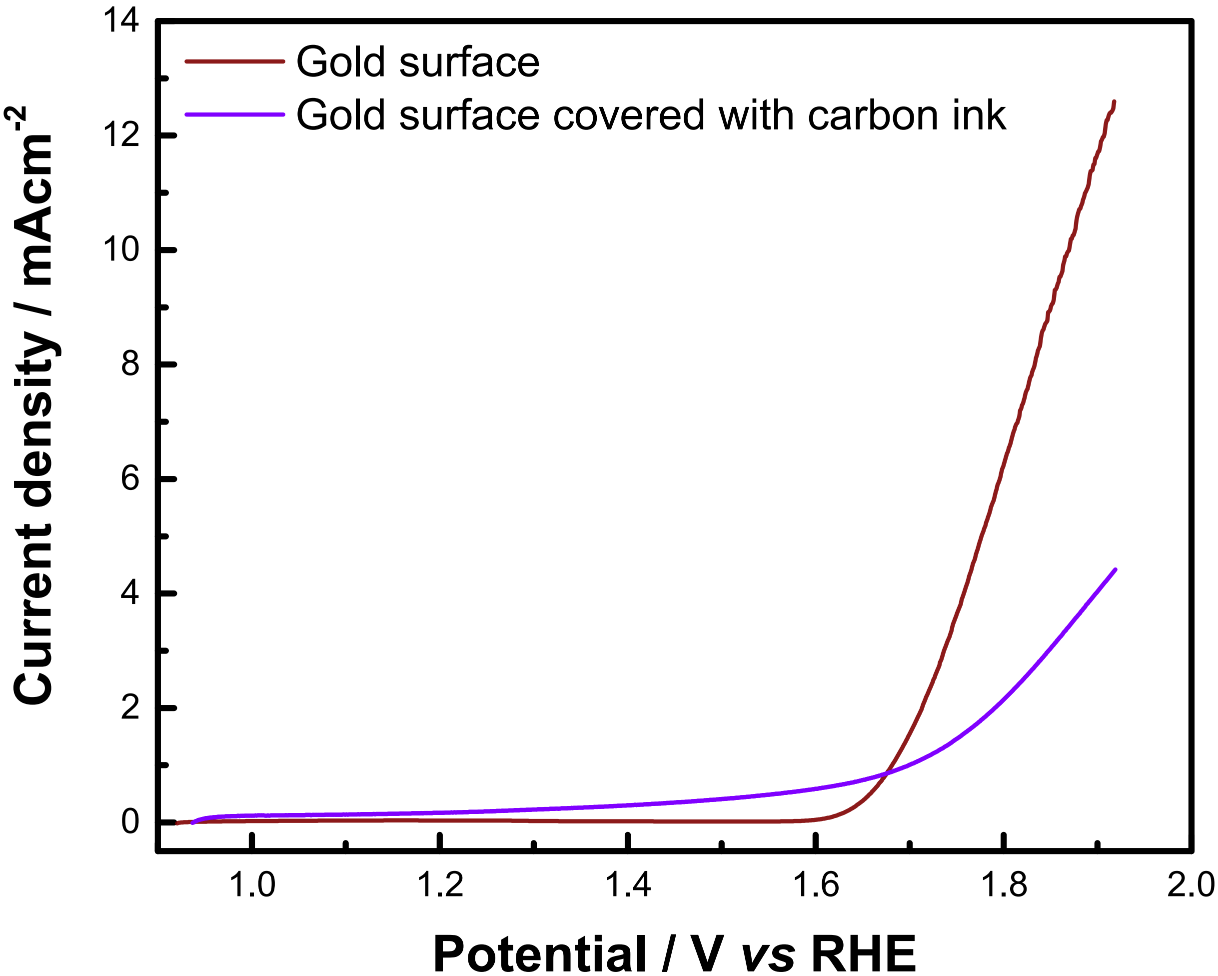

Figure S3. Rotating disc electrode voltammetry curves for the oxygen evolution for Gold electrode (wine) and gold electro covered by carbon ink (violet).

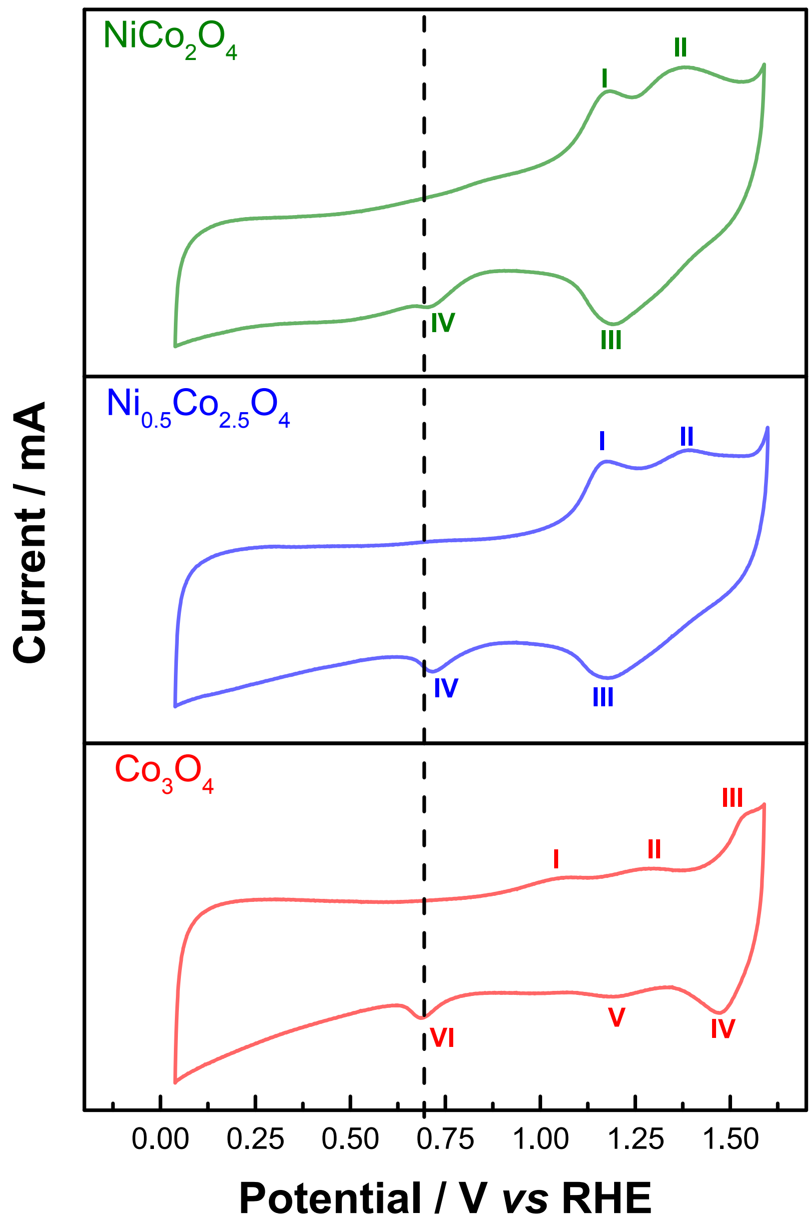

Figure S4. Electrochemical profiles of Co_3O_4 (red), $Ni_{0.5}Co_{2.5}O_4$ (blue) and $NiCo_2O_4$ (green).

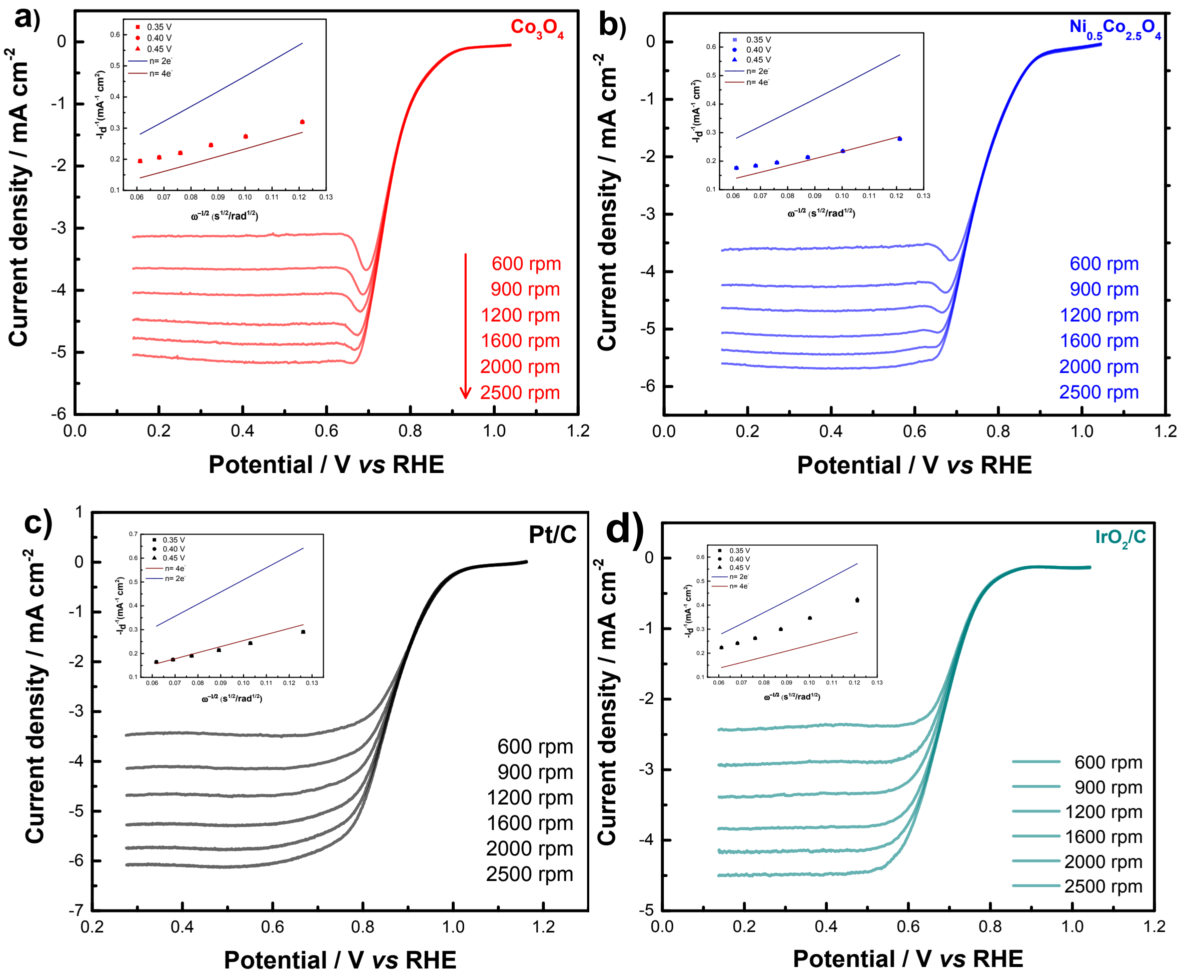

Figure S5 Rotating disc electrode voltammetry curves for the oxygen reduction reaction (ORR) in an alkaline medium (0.1 M KOH) and K-L plots (insets) for a) Co_3O_4, b) $Ni_{0.5}Co_{2.5}O_4$, c) Pt/C and d) IrO_2/C.

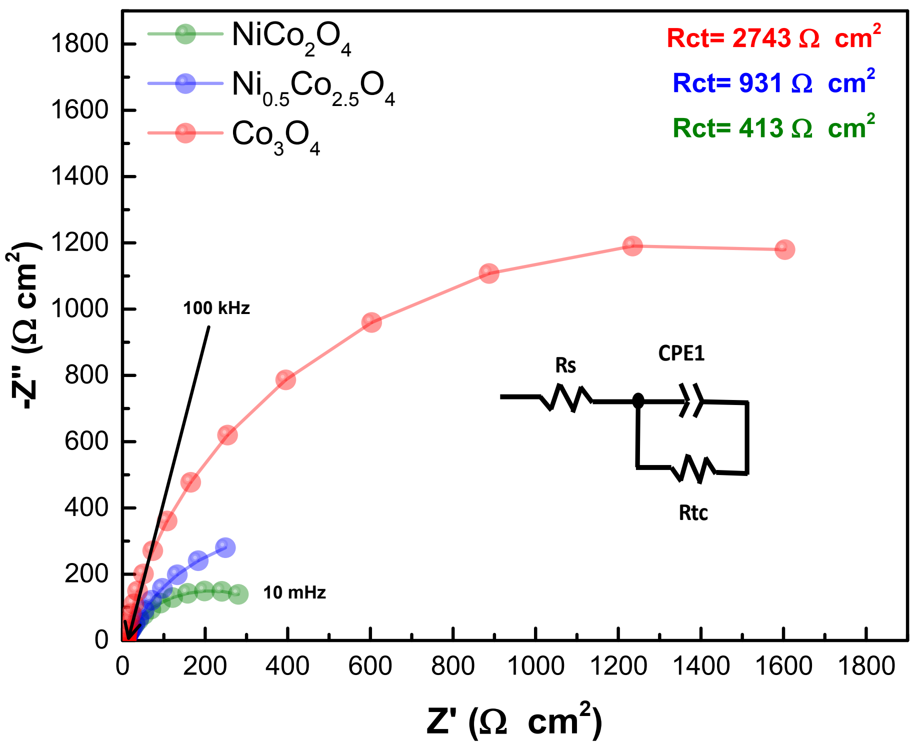

Figure S6. Nyquist plots obtained at 0.84 V *vs*. RHE for frequencies ranging from 100 kHz to 0.01 Hz. The experiment was performed using 0.1 M KOH as the electrolyte.

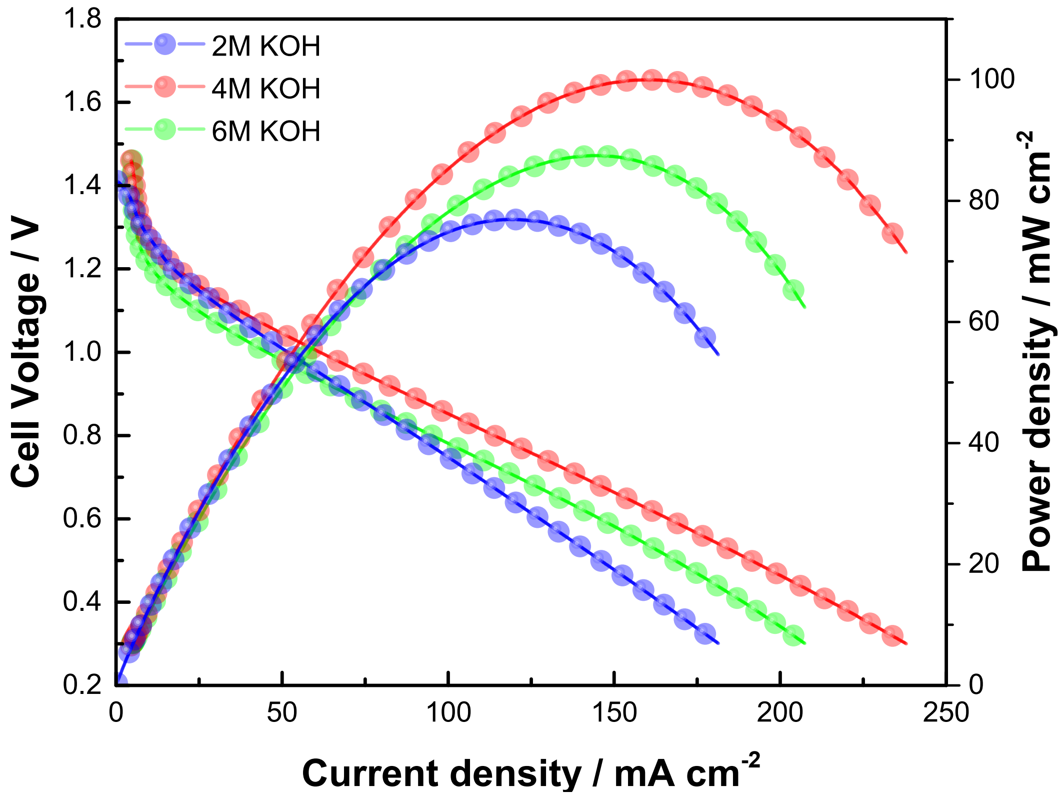

Figure S7. Polarization and power densities curves for $NiCo_2O_4$ at different KOH concentrations.

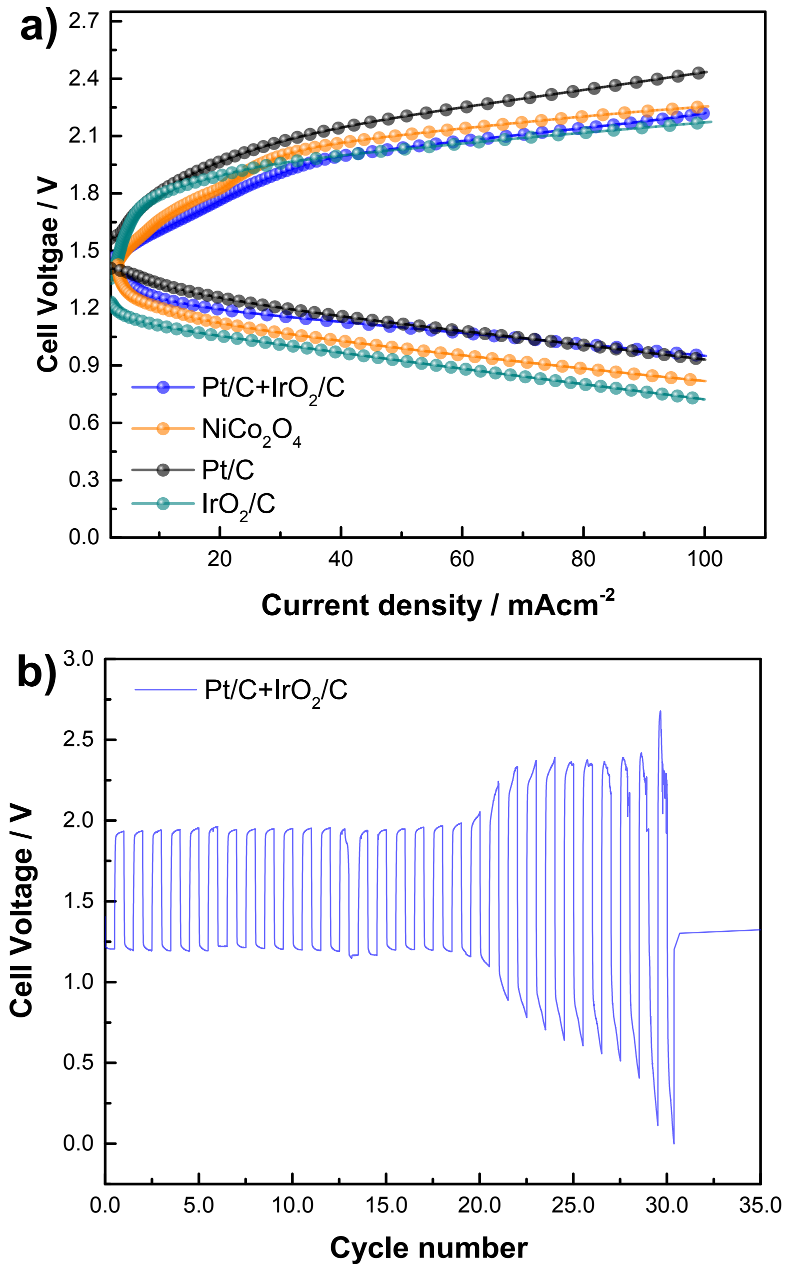

Figure S8. a) Charging and discharging polarization curves of Zn-air batteries operated with $NiCo_2O_4$ 3DOM spinel, and benchmarked Pt/C, IrO_2/C and Pt/C + IrO_2/C air electrocatalysts. b) Charge/discharge cycling curves of rechargeable ZAB at 10 mA cm^{-2} using Pt/C + IrO_2/C.

Table S1. Physicochemical characteristics for 3DOM materials determined from X–ray diffraction.

Peak	Experimental position Co_3O_4	Experimental position $Ni_{0.5}Co_{2.5}O4$	Experimental position $NiCo_2O_4$	d-spacing Co_3O_4 (nm)	d-spacing $Ni_{0.5}Co_{2.5}O_4$ (nm)	d-spacing $NiCo_2O_4$ (nm)	Reported peak position Co_3O_4	Reported d-spacing of Co_3O_4 (nm)	Reported peak position $NiCo_2O_4$	Reported d-spacing of $NiCo_2O_4$
(111)	18.74	18.92		0.4668	0.4624		19.06	0.4651	18.90	0.4690
(220)	31.15	31.12	30.70	0.2830	0.2833	0.2871	31.38	0.2848	31.14	0.2869
(311)	36.65	36.74	36.23	0.2417	0.2411	0.2444	36.97	0.2429	36.69	0.2447
(222)	38.38	38.67	37.93	0.2312	0.2295	0.2338	38.68	0.2325	38.40	0.2342
(400)	44.62	44.77	44.24	0.2002	0.1995	0.2018	44.97	0.2014	44.52	0.2029
(422)	55.51	55.15	55.06	0.1631	0.1641	0.1644	55.86	0.1644	55.44	0.1656
(511)	59.23	59.23	58.72	0.1537	0.1537	0.1550	59.58	0.1550	59.09	0.1562
(440)	65.25	63.03	64.76	0.1411	0.1413	0.1419	65.49	0.1424	64.98	0.1434
(533)	77.38	77.32	76.75	0.1215	0.12165	0.1224	77.66	0.1228	77.54	0.1230

Table S2. Elemental composition obtained by EDS of a) $Ni_{0.5}Co_{2.5}O_4$, and b) $NiCo_2O_4$

a)

Element	At. No.	Netto	Mass [%]	Mass Norm. [%]	Atom [%]	abs. error [%] (1 sigma)	rel. error [%] (1 sigma)
Nickel	28	12374	2.89	3.51	1.10	0.10	3.53
Cobalt	27	56260	11.33	13.75	4.27	0.32	2.78
Oxygen	8	12565	68.16	82.73	94.63	9.27	13.61
		Sum	**82.39**	**100.00**	**100.00**		

b)

Element	At. No.	Netto	Mass [%]	Mass Norm. [%]	Atom [%]	abs. error [%] (1 sigma)	rel. error [%] (1 sigma)
Nickel	28	65522	6.39	6.28	1.97	0.19	2.90
Cobalt	27	140552	11.71	11.52	3.59	0.32	2.75
Oxygen	8	36093	83.56	82.20	94.44	10.14	12.14
		Sum	**101.66**	**100.00**	**100.00**		

Table S3. Elemental composition obtained by XPS for Co_3O_4, $Ni_{0.5}Co_{2.5}O_4$ and $NiCo_2O_4$.

Sample	Specie	Weight % (Experimental)	Weight % (Theorical)	Atomic % (Experimental)	Atomic % (Theorical)
Co_3O_4	Co 2p	69.71	73.42	33.16	42.86
	O 1s	30.29	26.58	66.84	57.14
$Ni_{0.5}Co_{2.5}O_4$	Co 2p	46.88	42.09	15.70	35.72
	O 1s	39.00	41.14	79.97	57.14
	Ni 2p	14.12	16.77	4.33	7.14
$NiCo_2O_4$	Co 2p	38.37	49.00	14.07	28.58
	O 1s	37.55	26.60	80.50	57.14
	Ni 2p	24.08	24.40	5.43	14.28

Table S4. ORR performance using 3DOM spinels, and benchmarked Pt/C and IrO_2/C.

Catalyst	E_{onset} (V vs RHE)	$E_{1/2}$ (V vs. RHE)	Limit current density (mA cm^{-2})
Co_3O_4	0.91	0.74	4.41
$Ni_{0.5}Co_{2.5}O_4$	0.94	0.75	5.10
$NiCo_2O_4$	0.95	0.77	5.11
Pt/C	1.03	0.85	5.25
IrO2/C	0.89	0.69	3.70

Table S5. Activity comparison of the 3DOM spinels with other recently reported spinel materials for the ORR and OER.

Catalyst	ORR $E_{1/2}$ (V *vs.* RHE)	OER at 10 mA cm^{-2} (V *vs.* RHE)	ΔE ($E_{OER}-E_{ORR}$) (V)	Catalyst mass loading (mg cm^{-2})	Ref.
$NiCo_2O_4$	0.77	1.64	0.87	0.27	This work
$Ni_{0.5}Co_{2.5}O_4$	0.75	1.71	0.96	0.27	This work
Co_3O_4	0.74	1.75	1.01	0.27	This work
NiCo-Air	0.74	1.67	0.93	0.28	1
Co_3O_4/Co_2MnO_4 nanocomposite	0.68	1.77	1.09	0.20	2
Co_3ZnC/Co@CN	0.73	1.60	0.87	0.20	3
Fe/N-CNTs	0.81	1.75	0.94	0.20	4
$Mn_2O_3+Co_3O_4$	0.74	1.64	0.90	0.10	5
Flower-like $NiCo_2O_4$	0.74	1.64	0.90	0.31	6
$NiCo_2O_4/C$	0.71	1.67	0.96	0.15	7
Ni/NiO/ $NiCo_2O_4$/ N-CNT-As	0.74	1.60	0.86	0.24	8
$NiCo_2O_4$	0.75	1.72	0.97	-	9
$NiCo_2O_4$-G	0.54	1.67	1.13	0.41	10
NCO-N2	0.76	1.62	0.86	-	11
$NiCo_2O_4$/CNTs	0.73	1.61	0.88	0.25	12
$NiCo_2O_4$@N-CNWs	0.80	1.56	0.76	0.25	13
$NiCo_2O_4$ rosettes-like	0.75	1.69	0.94	0.40	14

CN= Nitrogen doped graphene layer,

N-CNTs= Nitrogen-doped carbon nanotubes

N-CNT-As= N-doped carbon nanotube aerogels

G= Graphene sheets

CNTs= Carbon nanotubes

N-CNWs= N- doped carbon nanowebs

References

1 W. Liu, J. Bao, L. Xu, M. Guan, Z. Wang, J. Qiu and Y. Huang, *Appl. Surf. Sci.*, 2019, **478**, 552–559.

2 D. Wang, X. Chen, D. G. Evans and W. Yang, *Nanoscale*, 2013, **5**, 5312–5315.

3 J. Su, G. Xia, R. Li, Y. Yang, J. Chen, R. Shi, P. Jiang and Q. Chen, *J. Mater. Chem. A*, 2016, **4**, 9204–9212.

4 Y. Liu, H. Jiang, Y. Zhu, X. Yang and C. Li, *J. Mater. Chem. A*, 2016, **4**, 1694–1701.

5 W. Wang, L. Kuai, W. Cao, M. Huttula, S. Ollikkala, T. Ahopelto, A. P. Honkanen, S. Huotari, M. Yu and B. Geng, *Angew. Chemie - Int. Ed.*, 2017, **56**, 14977–14981.

6 Y. Li, Z. Zhou, G. Cheng, S. Han, J. Zhou and J. Yuan, *Electrochim. Acta*, 2020, **341**, 135997.

7 J. Wang, Z. Wu, L. Han, R. Lin, H. L. Xin and D. Wang, *ChemCatChem*, 2016, **8**, 736–742.

8 N. Ma, Y. Jia, X. Yang, X. She, L. Zhang, Z. Peng, X. Yao and D. Yang, *J. Mater. Chem. A*, 2016, **4**, 6376–6384.

9 Z. Y. and R. Y. Chao Jin, Fanliang Lu, Xuecheng Cao, *J. Mater. Chem. A*, 2013, **1**, 12170–12177.

10 D. U. Lee, B. J. Kim and Z. Chen, *J. Mater. Chem. A*, 2013, **1**, 4754–4762.

11 M. Prabu, K. Ketpang and S. Shanmugam, *Nanoscale*, 2014, **6**, 3173–3181.

12 X. Xiao, X. Li, J. Wang, G. Yan, Z. Wang, H. Guo and Y. Liu, *Ceram. Int.*, 2020, **46**, 6262–6269.

13 H. Ge, G. Li, T. Zheng, F. Wang, M. Shao and H. Liu, *Electrochim. Acta*, 2019, **319**, 1–9.

14 J. Béjar, L. Álvarez-Contreras, J. Ledesma-García, N. Arjona and L. G. Arriaga, *J. Electroanal. Chem.*, 2019, **847**, 113190.